

# Radiation dose reduction for coronary artery calcium scoring at 320-detector CT with adaptive iterative dose reduction 3D

Fuminari Tatsugami<sup>1</sup> · Toru Higaki<sup>1</sup> · Wataru Fukumoto<sup>1</sup> · Yoko Kaichi<sup>1</sup> · Chikako Fujioka<sup>2</sup> · Masao Kiguchi<sup>2</sup> · Hideya Yamamoto<sup>3</sup> · Yasuki Kihara<sup>3</sup> · Kazuo Awai<sup>1</sup>

Received: 8 January 2015 / Accepted: 5 March 2015 / Published online: 10 March 2015  
© Springer Science+Business Media Dordrecht 2015

**Abstract** To assess the possibility of reducing the radiation dose for coronary artery calcium (CAC) scoring by using adaptive iterative dose reduction 3D (AIDR 3D) on a 320-detector CT scanner. Fifty-four patients underwent routine- and low-dose CT for CAC scoring. Low-dose CT was performed at one-third of the tube current used for routine-dose CT. Routine-dose CT was reconstructed with filtered back projection (FBP) and low-dose CT was reconstructed with AIDR 3D. We compared the calculated Agatston-, volume-, and mass scores of these images. The overall percentage difference in the Agatston-, volume-, and mass scores between routine- and low-dose CT studies was 15.9, 11.6, and 12.6 %, respectively. There were no significant differences in the routine- and low-dose CT studies irrespective of the scoring algorithms applied. The CAC measurements of both imaging modalities were highly correlated with respect to the Agatston- ( $r = 0.996$ ), volume- ( $r = 0.996$ ), and mass score ( $r = 0.997$ ;  $p < 0.001$ , all); the Bland–Altman limits of agreement scores were  $-37.4$  to  $51.4$ ,  $-31.2$  to  $36.4$  and  $-30.3$  to  $40.9$  %, respectively, suggesting that AIDR 3D was a good alternative for FBP. The mean effective radiation dose for routine- and low-dose CT was 2.2 and 0.7 mSv, respectively. The use of AIDR 3D made it possible to reduce the

radiation dose by 67 % for CAC scoring without impairing the quantification of coronary calcification.

**Keywords** Coronary artery calcium · Iterative reconstruction · Dose reduction · 320-detector CT scanner

## Introduction

The coronary artery calcium (CAC) score measured on fast computed tomography (CT) scanners is an unequivocal marker of coronary atherosclerosis [1, 2]. However, the high quality of images obtained by multi-detector row CT comes at the expense of high radiation exposure; the reported dose for CAC scoring is between 1.4 and 2.0 mSv [3–5]. As its long-term effects are not well defined, the radiation dose must be kept at the minimum that allows adequate quantification of the CAC score.

Iterative reconstruction (IR) algorithms reduce the noise and improve the image quality [6–8]. The adaptive iterative dose reduction 3D (AIDR 3D) algorithm developed by Toshiba Medical Systems Corp. is commercially available; it reduces image noise and streak artifacts in the reconstruction domain. It is expected to lower the required radiation dose for a noise level similar to conventional filtered back projection (FBP) reconstruction while maintaining diagnostic image quality.

To our knowledge there are no studies that evaluated the possibility of a radiation dose reduction for CAC scoring using IR techniques determined by patient data. Therefore, to assess whether IR allows for a radiation dose reduction in patients undergoing CAC scoring we performed phantom- and clinical studies using a 320-detector CT scanner. The phantom study was performed as a precursor to determine the best dose reduction level for CAC scoring with

✉ Fuminari Tatsugami  
sa104@rg8.so-net.ne.jp

<sup>1</sup> Department of Diagnostic Radiology, Hiroshima University, 1-2-3 Kasumi, Minami-ku, Hiroshima 734-8551, Japan

<sup>2</sup> Department of Radiology, Hiroshima University, 1-2-3 Kasumi, Minami-ku, Hiroshima 734-8551, Japan

<sup>3</sup> Department of Cardiovascular Medicine, Hiroshima University, 1-2-3 Kasumi, Minami-ku, Hiroshima 734-8551, Japan

AIDR 3D. Based on the phantom study, a 67 % dose reduction was prescribed to the patient study. In the clinical study we compared the accuracy of the CAC score obtained with routine-dose CT reconstructed with FBP and low-dose CT reconstructed with AIDR 3D.

## Materials and methods

### Phantom study

We used a cardiac CT calibration phantom (QRM, Moehrendorf, Germany) with a  $200 \times 300$  mm body diameter and a 100 mm depth that designed as a calibration standard for the quantification of coronary calcium (Fig. 1). Its body includes artificial lungs and a spine insert surrounded by a material mimicking soft tissue. At the position of the heart there is a 100-mm diameter cylindrical hole for the placement of a calibration insert containing three sets of calcified cylinders measuring 1-, 3-, and 5 mm in both diameter and height whose calcium hydroxyapatite (CaHA) density equals 200-, 400-, and 800 mg/cm<sup>3</sup>, respectively (Fig. 1).

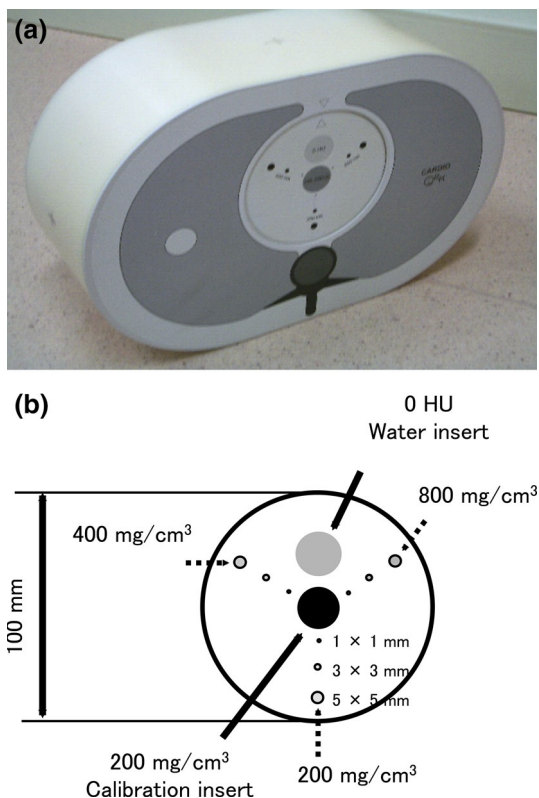


**Fig. 1** **a** Photograph of the anthropomorphic phantom body with the calibration insert. **b** Diagram of the frontal view of the calibration insert with 9 different calcifications and 2 large calibration inserts (0-HU water and 200 mg/cm<sup>3</sup> calcium hydroxyapatite)

We used a 320-detector CT scanner (Aquilion ONE, Toshiba Corp. Medical Systems, Tokyo, Japan) with prospective ECG-triggering. The scanning parameters were tube potential, 120 kVp; rotation time, 0.35 s. Images were reconstructed using a medium-smooth kernel (FC14); the slice thickness was 3 mm without overlap. Images were obtained at tube currents of 150-, 100-, 70-, 50-, and 40 mA; the standard deviation (SD) of the CT values at the images reconstructed with FBP corresponds to 20-, 25-, 30-, 35-, and 40 Hounsfield units (HU). Axial images were reconstructed for each CT study with AIDR 3D using vendor-recommended settings (preset “standard” of 3 options, i.e. mild, standard, and strong) and FBP. Five scans were obtained in each series. In this phantom study, the image noise and CAC scores obtained at 150 mA with FBP were defined as the reference data.

The Agatston score was defined by the presence of more than two adjacent pixels with HU values greater than 130 [9]. Lesions were automatically identified and marked in color on the workstation (Virtual Place ver. 3.3; Aze, Tokyo, Japan). We also calculated the calcium volume and mass score as they were reported to reduce inter- and intraobserver variability [10–12]. The volume score was compiled by automatic multiplication of the coronary artery calcium area on axial slices by the slice thickness. The mass score was calculated with the equation [10–12]:  $\text{mass score} = \sum (\text{area} \times \text{slice increment} \times \text{mean CT density}) \times \text{calibration factor}$ . To obtain the calcium mass we calculated the calibration factor by measuring the attenuation of the large calcium hydroxyapatite calibration insert at 200 mg/cm<sup>3</sup> and the water insert; the calibration factor on our CT scanner was 0.701311. All CAC scores were obtained for all CT studies.

### Patient study

This study was performed in compliance with the principles of the Declaration of Helsinki and approved by our institutional review board. Informed prior consent was obtained from all patients.

We recruited 71 consecutive patients who were referred for coronary CT angiography between September and December 2013. In 56 patients coronary artery disease (CAD) was suspected to be due to dyspnea ( $n = 11$ ), typical angina pectoris ( $n = 13$ ), atypical chest pain ( $n = 25$ ), or high cardiovascular risk ( $n = 7$ ). The other 15 had known CAD; they were referred for stent patency ( $n = 8$ ) or follow-up after myocardial infarction ( $n = 7$ ). Our inclusion criteria required a diagnostic study with an Agatston score greater than zero. Patients were excluded if they had a history of cardiac surgery ( $n = 6$ ), coronary stents ( $n = 8$ ), or a pectoral transvenous pacemaker ( $n = 3$ ). Consequently, 54 patients (39 men, 15 women;

median age 70 years; range 44–86 years) were enrolled in this study.

### CT scanning

All CT studies were performed using a 320-detector CT scanner with prospective ECG-triggering during a single heart beat. Patients whose resting heart rate exceeded 65 beats per minute (bpm) perorally received 20–40 mg of metoprolol (Seloken; AstraZeneca, Zoetermeer, Netherlands) 60 min before undergoing CT.

Each patient underwent two consecutive CT examinations for CAC scoring. For the first CT study (routine-dose CT) tube current was determined as follows; after a localizer radiograph acquisition, we simulated the tube current at which the standard deviation (noise level) of the heart was that obtained at 20 HU at the images reconstructed with FBP, using the z-axis modulation technique (Volume E.C., Toshiba Medical, Tokyo, Japan). For the second study (low-dose CT) we used one-third of the tube current applied for routine-dose CT; this reduction rate of the tube current was based on the results of our phantom study. The patients remained on the table during the two examinations without changing their position. In all examinations the phase window during which the patient was exposed was limited to 75 % of the R–R interval. The other scanning parameters, identical in both examinations, were: tube potential, 120 kVp; rotation time, 0.35 s; z-coverage, 120–160 mm.

Images were reconstructed using a medium-smooth kernel (FC14), a matrix size of  $512 \times 512$ , and a slice thickness of 3 mm without overlap. The images obtained with routine-dose CT were reconstructed with FBP; low-dose CT images with FBP or AIDR 3D using the standard level. Reconstructed image data were transferred to a computer workstation (Virtual Place ver. 3.3; Aze, Tokyo, Japan) for post-processing.

### Quantitative analysis

The Agatston-, volume-, and mass scores were recorded by one reader with 8 years of experience in cardiovascular radiology. All CAC scoring was performed in each routine- and low-dose CT study.

For risk stratification the patients were categorized based on their Agatston score of the routine-dose CT study. For group 1 (low risk) the cutoff value was 1–30, for group 2 (moderate risk) it was 31–100, for group 3 (moderately high risk) it was 101–400; group 4 (high risk) had a score greater than 400 [13].

Image noise was determined as the SD of the attenuation value in a region of interest placed in the left ventricle. The effective radiation dose for each CT study was calculated

as the product of the dose-length product (DLP) times a conversion coefficient for the chest ( $k = 0.014 \text{ mSv/mGy cm}$ ) [14].

### Statistical analyses

The effective radiation dose for routine- and low-dose CT was assessed with the two-tailed paired-samples *t* test. The percent difference in the CAC scores obtained in routine-dose CT studies with FBP and in low-dose CT studies with AIDR 3D was calculated using the formula [13]:  $\text{abs}(A - B)/(0.5 \times A + 0.5 \times B) \times 100 \%$ . The correlation of the scoring algorithms applied in the two studies was determined with the Pearson correlation coefficient. Bland–Altman plots were constructed for each scoring algorithm to assess agreement between the scores obtained in the two studies. Percent differences between the scores of the two studies were plotted against their average scores.

Data analysis was with MedCalc (version 11.3, MedCalc Software). For all statistical analyses,  $p < 0.05$  was considered to indicate a significant difference.

## Results

### Phantom study

Agatston scores at various calcium size and CaHA density calculated from images reconstructed with FBP and AIDR 3D are shown in Table 1. Agatston scores for small (Calcium diameter of 1 mm) or low density (CaHA density of  $200 \text{ mg/cm}^3$ ) inserts tended to decrease with AIDR3D compared to those reconstructed with FBP; those of median size (Calcium diameter of 3 mm) or median density (CaHA density of  $400 \text{ mg/cm}^3$ ) inserts remained unchanged with AIDR 3D; those of large (Calcium diameter of 5 mm) or high density (CaHA density of  $800 \text{ mg/cm}^3$ ) inserts tended to increase at low dose scan (40–70 mA) with AIDR 3D.

The image noise and the Agatston-, volume-, and mass scores calculated from images reconstructed with FBP or AIDR 3D are shown in Table 2. The mean image noise acquired at 40 mA and reconstructed with AIDR 3D was comparable to the values obtained at 150 mA and reconstructed with FBP; the mean Agatston score obtained at 50 mA with AIDR 3D was comparable to that at 150 mA with FBP; the mean volume and mass scores obtained at 70 mA with AIDR 3D were comparable to those at 150 mA with FBP. Regarding the mean volume and mass scores, the difference values obtained at 70- and 50 mA with AIDR 3D were very small ( $682.9$  vs.  $685.7 \text{ mm}^3$ ,  $183.8$  vs.  $186.0 \text{ mg}$ , respectively). Therefore we expected that with the aid of AIDR 3D the radiation dose could be

**Table 1** Phantom study: mean Agatston scores at various (a) calcium size, (b) calcium hydroxyapatite density calculated from images reconstructed with FBP and AIDR 3D

	FBP	AIDR 3D (Standard)				
	150 mA	150 mA	100 mA	70 mA	50 mA	40 mA
(a) Calcium diameter						
1 (mm)	4.1	2.5	2.8	2.3	2.0	2.4
3 (mm)	176.9	173.3	175.4	176.7	173.7	175.5
5 (mm)	644.8	632.3	646.12	663.3	654.12	685.1
(b) CaHA density						
200 (mg/cm <sup>3</sup> )	144.7	132.6	140.4	142.4	132.1	148.7
400 (mg/cm <sup>3</sup> )	286.6	282.8	288.0	291.7	290.9	298.9
800 (mg/cm <sup>3</sup> )	394.4	392.8	395.9	404.5	406.8	414.1

FBP filtered back projection, AIDR 3D adaptive iterative dose reduction 3D, CaHA calcium hydroxyapatite

**Table 2** Phantom study: mean image noise and calcium scores calculated from images reconstructed with FBP and AIDR 3D

	FBP	AIDR 3D (standard)				
	150 mA	150 mA	100 mA	70 mA	50 mA	40 mA
Image noise (HU)	21.1	13.5	14.6	16.7	19.6	20.4
Agatston score (mm <sup>2</sup> )	825.2	803.5	821.3	837.9	827.6	856.5
Volume score (mm <sup>3</sup> )	679.7	661.6	667.6	682.9	685.7	707.3
Mass score (mg)	184.5	180.5	178.8	183.8	186.0	190.5

FBP filtered back projection, AIDR 3D adaptive iterative dose reduction 3D

reduced by 67 % (from 150 to 50 mA) in clinical studies of CAC

### Patient study

The mean BMI of the study population ( $n = 54$ ) was  $23.9 \pm 3.3$  (range 17.2–31.6); 3 patients (5.6 %) were underweight (BMI < 18.5), 32 (59.3 %) were of normal weight (BMI 18.5–24.9), 17 (31.5 %) were overweight (BMI 25–29.9), and 2 (3.7 %) were obese (BMI > 30). The mean tube current at routine- and low-dose CT were 315.0 and 103.6 mA ( $p < 0.01$ ). The mean DLP and effective radiation dose at routine-dose CT were 156.5 mGy  $\times$  cm and 2.2 mSv; at low-dose CT they were 49.9 mGy  $\times$  cm and 0.7 mSv ( $p < 0.01$ ). The mean Agatston-, volume-, and mass scores and mean image noise obtained at routine- and low-dose CT are shown in Table 3. The mean image noise was similar at low-dose CT with AIDR 3D and routine-dose CT with FBP ( $p = 0.82$ ). There was no patient whose calcification

disappeared (Agatston score = 0) at low-dose CT scans with AIDR 3D.

The overall percentage difference in the Agatston-, volume-, and mass scores between routine-dose CT with FBP and low-dose CT with AIDR 3D was 15.9, 11.6, and 12.6 % respectively. The absolute percentage difference in the CAC scores based on the risk level is shown in Table 4. The lower the amount of calcium present the higher was the percentage difference.

The Agatston score obtained at low-dose CT scans with AIDR 3D strongly correlated with the score obtained for routine-dose CT scans with FBP ( $r = 0.996$ ,  $p < 0.001$ ) (Fig. 2a) and the volume- and mass scores obtained with low-dose CT scans with AIDR 3D strongly correlated with the scores on routine-dose CT scans with FBP ( $r = 0.996$ ,  $p < 0.001$ ;  $r = 0.997$ ,  $p < 0.001$ , respectively; Fig. 2b, c).

Comparison of the results of Bland–Altman analysis of the Agatston-, volume-, and mass scores obtained with low-dose CT with AIDR 3D and routine-dose CT with FBP revealed no systemic bias (Fig. 3). The Bland–Altman

**Table 3** Clinical study: mean image noise and coronary artery calcium scores obtained with routine- and low-dose CT

	RDCT with FBP	LDCT with FBP	LDCT with AIDR 3D
Image noise (HU)	20.8	36.6	20.7
Agatston score (mm <sup>2</sup> )	361.6	393.7	356.8
Volume score (mm <sup>3</sup> )	294.7	328.2	293.8
Mass score (mg)	65.6	72.0	64.0

FBP filtered back projection, AIDR 3D adaptive iterative dose reduction 3D, RDCT Routine-dose CT, LDCT Low-dose CT

**Table 4** Absolute percentage differences in the coronary artery calcium scores of patients in different risk categories

	Group 1 (scores 1–30)	Group 2 (scores 31–100)	Group 3 (scores 101–400)	Group 4 (scores > 400)
No. of patients	6	10	20	17
Agatston score (mm <sup>2</sup> )	42.0	27.5	11.3	5.4
Volume score (mm <sup>3</sup> )	29.5	16.1	10.0	4.7
Mass score (mg)	33.5	20.3	8.3	6.1

Comparison was between routine-dose CT with FBP and low-dose CT with AIDR 3D

FBP filtered back projection, AIDR 3D adaptive iterative dose reduction 3D

limits of agreement for the Agatston-, volume-, and mass scores were  $-37.4$  to  $51.4$  %,  $-31.2$  to  $36.4$  %, and  $-30.3$  to  $40.9$  %, respectively, suggesting that AIDR 3D was a good alternative for FBP. A representative case is shown in Fig. 4.

## Discussion

In the first study to assess the possibility of reducing the radiation exposure for CAC scoring by using AIDR 3D on a 320-detector CT scanner we document that AIDR 3D facilitates a decrease in the radiation exposure by 67 % compared to studies that use the dose currently applied and FBP.

There has been considerable interest in reducing the tube current (mA) for CAC scoring [15–18] because the patient radiation dose is directly and linearly related to the applied tube current [19]. There was no significant difference in the CAC score when low/high tube currents of 55 mAs/165 mAs [18] and 40 mAs/150 mAs [20] were applied. However, when the tube current is too low, the increased image noise manifests as small focal areas of high attenuation that can simulate or accentuate focal calcified arterial plaques [21].

AIDR 3D is a hybrid IR technique that can be used clinically. AIDR 3D algorithm applies noise reduction techniques to the raw data and image domains. AIDR 3D efficiently eliminates noise and streak artifact due to photon starvation with a statistical noise and scanner model considering both photon and electronic noise in the raw data domain. The raw data are reconstructed with FBP then a sophisticated iterative technique that optimizes reconstructions for the particular region is applied in the image domain, resulting noise reduction while preserving spatial resolution and image texture [22]. It drastically reduces the image noise compared with FBP reconstruction and the additional time required for calculations is clinically acceptable. In CT coronary angiography, AIDR 3D can help to reduce the radiation dose by 22–50 % [23, 24]. Therefore we posited that AIDR 3D held promise for reducing the radiation exposure for clinical CAC scoring.

The effect of IR techniques on CAC scoring has been reported [25, 26]. van Osch et al. [26] found that the Agatston-, volume-, and mass scores were lower on adaptive statistical iterative reconstruction (ASIR)- than FBP images and that the number of patients with a calcium score of zero increased by 13 % with 100 % ASIR. Kurata et al. [25] reported that the Agatston-, volume-, and mass scores decreased in proportion with the amount of sino-gram-affirmed iterative reconstruction (SAFIRE) and that high-grade SAFIRE resulted in the disappearance of detectable calcium in 3 of 70 patients with a low calcium burden. Based on these previous reports, we selected the “standard setting” of the AIDR 3D algorithm, not the “strong setting” of the AIDR 3D; no calcifications disappeared (Agatston score = 0) with that AIDR 3D setting.

In our phantom study, we evaluated the Agatston scores at various calcium size and CaHA density calculated from images reconstructed with FBP and AIDR 3D. Agatston scores for small or low density inserts tended to decrease with AIDR3D compared to those reconstructed with FBP, while Agatston scores for large or high density inserts tended to increase at low dose scan (40–70 mA) with AIDR 3D. Thus, large or high density inserts might have more dose reduction potential than small or low density inserts.

Based on our phantom study we expected that with AIDR 3D it would be possible to reduce the radiation dose by 67 % in patients undergoing CAC measurements. The mean image noise for low-dose CT with AIDR 3D (20.7 HU) and routine-dose CT with FBP (20.8 HU) was comparable; with both techniques the image noise level was acceptable for the evaluation of CAC (<20 HU) [27]. Also, low-dose CT with AIDR 3D and routine-dose CT with FBP yielded equivalent CAC measurements. Our results indicate that accurate quantification of calcium in the coronary artery is possible with AIDR 3D at an effective dose of 0.7 mSv, a radiation dose lower than in earlier reports (1.4–2.0 mSv) [3–5].

In our study the overall percentage difference (reproducibility) between routine- and low-dose CT (Agatston score, 15.9 %; volume score, 11.6 %; mass score, 12.6 %) was almost the same as in earlier reports (11–28, 9–12,

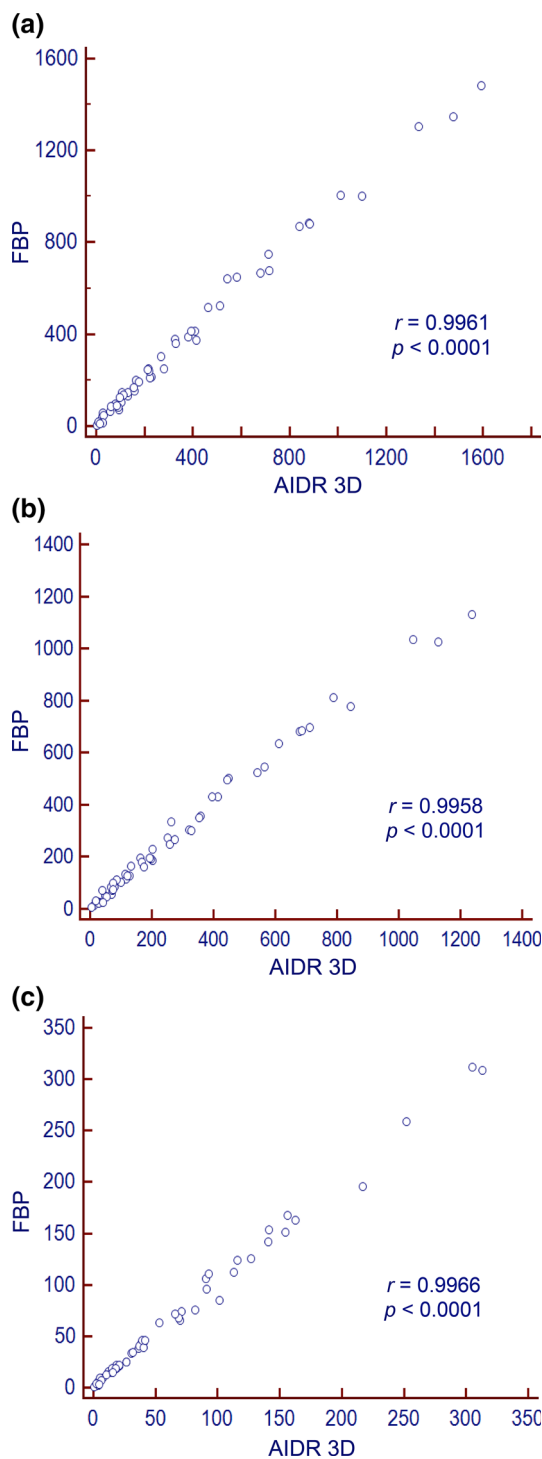


**Fig. 2** Scatter plots showing the correlation between CAC scores obtained at routine-dose CT with FBP and low-dose CT with AIDR 3D. **a** Strong correlation between the Agatston scores obtained at low-dose CT with AIDR 3D and routine-dose CT with FBP (Pearson correlation,  $r = 0.996$ ,  $p < 0.001$ ). **b** Strong correlation between volume scores obtained at low-dose CT with AIDR 3D and routine-dose CT with FBP ( $r = 0.996$ ,  $p < 0.001$ ). **c** Strong correlation between mass scores obtained at low-dose CT with AIDR 3D and routine-dose CT with FBP ( $r = 0.997$ ,  $p < 0.001$ )

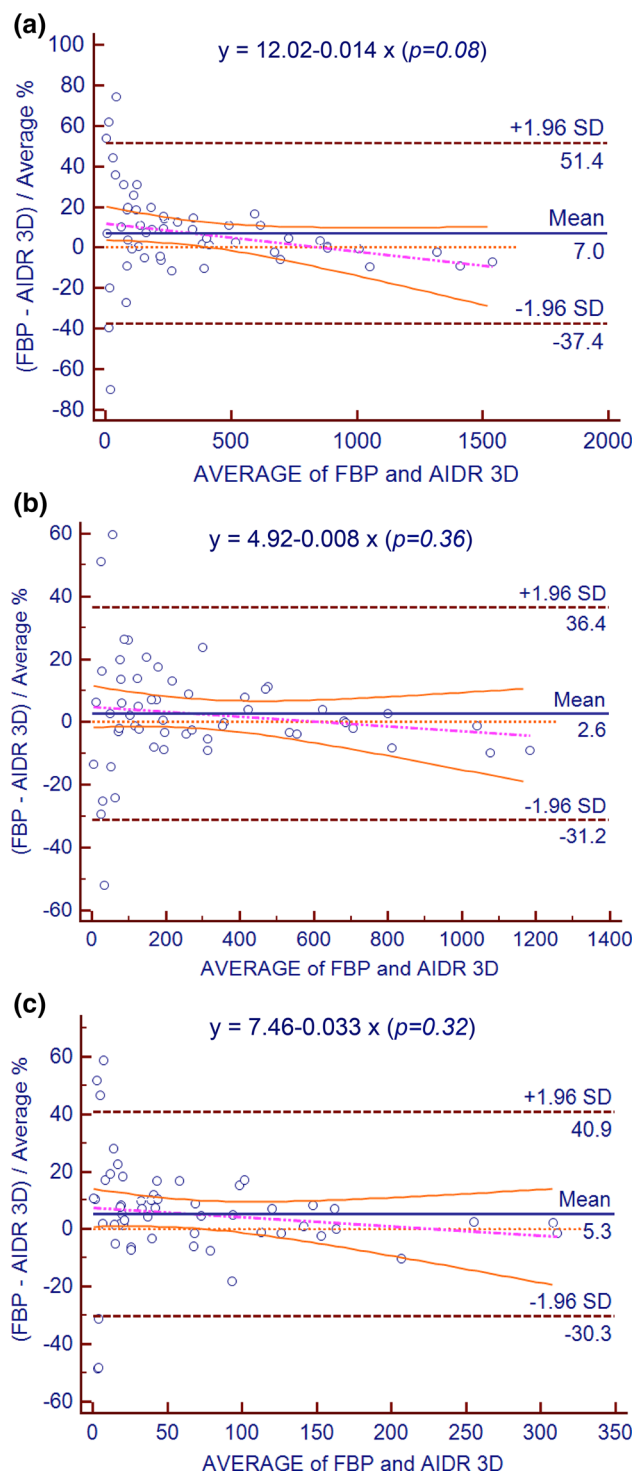


**Fig. 3** Bland–Altman analysis of the **a** Agatston-, **b** volume-, and **c** mass scores obtained in the two CT studies showed that there were no systemic biases. The Bland–Altman limits of agreement for the Agatston-, volume-, and mass scores were  $-37.4$  to  $51.4$  %,  $-31.2$  to  $36.4$  % and  $-30.3$  to  $40.9$  %, respectively

7–12 %) [13, 28, 29]. On the other hand, as the extent of calcification significantly affects reproducibility; the lower the amount of calcium present, the larger is the absolute

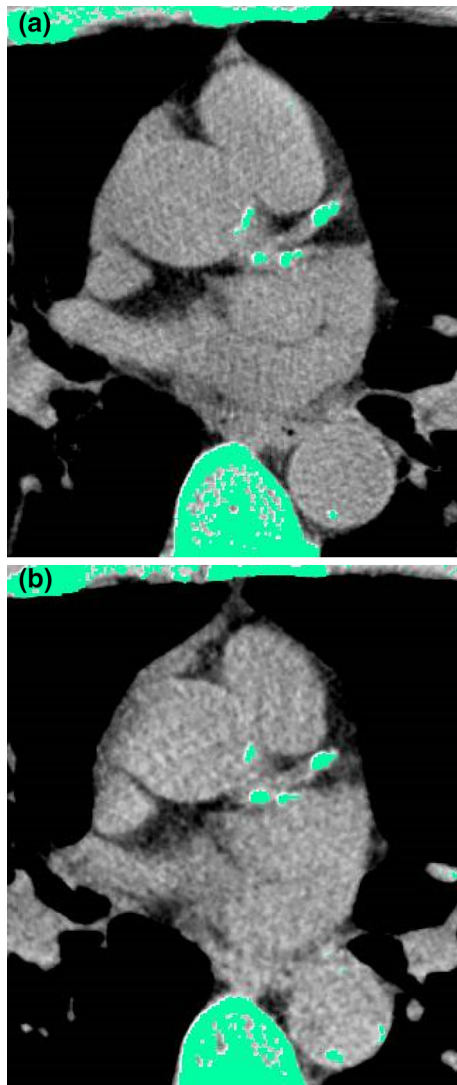


**Fig. 4** A 76-year-old man. Transverse CT images were obtained at the level of the left main artery branches at different tube currents but similar image noise. **a** CT images obtained at 180 mA and reconstructed with FBP (image noise, 19.6 HU; Agatston score, 666.5). **b** CT images obtained at 60 mA and reconstructed with AIDR 3D (image noise, 19.5 HU; Agatston score, 680.6)

percentage difference. For lower CAC scores the reported absolute percentage difference was 43–72 % [13, 30, 31]. Ours was slightly better (42 % in the low-risk group with an Agatston score of 1–30). We hypothesize that if the percentage difference in patients with lower CAC scores is large, the score itself is so low that it would not affect the patient's risk assessment.

Our study has some limitations. The small number of patients limits the informational value of our findings and additional investigations on larger patient populations are underway to confirm our preliminary results. Second, the mean body weight of our patients is lower than in average American and European subjects and studies are needed to

determine whether our results apply to heavier patients. Third, we performed CAC scoring on the same workstation to minimize the potential bias of different workstations. On different workstations the scores may differ slightly. Lastly, we investigated the effect of a specific IR algorithm on specific CT studies. The effect of other IR algorithms on different CT investigations may be different.

In conclusion, AIDR 3D can reduce the radiation exposure of patients undergoing CAC scoring by 67 % compared with the dose currently applied with FBP.

**Conflict of interest** Dr. Kazuo Awai is currently receiving a research grant from Toshiba Medical Systems, Ltd. The remaining authors of this manuscript declare no relationships with any companies, whose products or services may be related to the subject matter of the article.

## References

1. Wexler L, Brundage B, Crouse J et al (1996) Coronary artery calcification: pathophysiology, epidemiology, imaging methods, and clinical implications. A statement for health professionals from the American Heart Association. Writing Group. *Circulation* 94:1175–1192
2. O'Rourke RA, Brundage BH, Froelicher VF et al (2000) American College of Cardiology/American Heart Association Expert Consensus document on electron-beam computed tomography for the diagnosis and prognosis of coronary artery disease. *Circulation* 102:126–140
3. Genders TS, Pugliese F, Mollet NR et al (2010) Incremental value of the CT coronary calcium score for the prediction of coronary artery disease. *Eur Radiol* 20:2331–2340
4. Glodny B, Helmelt B, Trieb T et al (2009) A method for calcium quantification by means of CT coronary angiography using 64-multidetector CT: very high correlation with Agatston and volume scores. *Eur Radiol* 19:1661–1668
5. van der Bijl N, de Bruin PW, Geleijns J et al (2010) Assessment of coronary artery calcium by using volumetric 320-row multidetector computed tomography: comparison of 0.5 mm with 3.0 mm slice reconstructions. *Int J Cardiovasc Imag* 26:473–482
6. Gervaise A, Osemont B, Lecocq S et al (2012) CT image quality improvement using adaptive iterative dose reduction with wide-volume acquisition on 320-detector CT. *Eur Radiol* 22(2):295–301
7. Hara AK, Paden RG, Silva AC et al (2009) Iterative reconstruction technique for reducing body radiation dose at CT: feasibility study. *AJR Am J Roentgenol* 193:764–771
8. Liu YJ, Zhu PP, Chen B et al (2007) A new iterative algorithm to reconstruct the refractive index. *Phys Med Biol* 52:L5–13
9. Agatston AS, Janowitz WR, Hildner FJ et al (1990) Quantification of coronary artery calcium using ultrafast computed tomography. *J Am Coll Cardiol* 15:827–832
10. Hong C, Becker CR, Schoepf UJ et al (2002) Coronary artery calcium: absolute quantification in nonenhanced and contrast-enhanced multi-detector row CT studies. *Radiology* 223:474–480
11. Hong C, Bae KT, Pilgram TK (2003) Coronary artery calcium: accuracy and reproducibility of measurements with multi-detector row CT—assessment of effects of different thresholds and quantification methods. *Radiology* 227:795–801
12. Hoffmann U, Siebert U, Bull-Stewart A et al (2006) Evidence for lower variability of coronary artery calcium mineral mass measurements by multi-detector computed tomography in a

- community-based cohort—consequences for progression studies. *Eur J Radiol* 57:396–402
13. Budoff MJ, Kessler P, Gao YL et al (2008) The interscan variation of CT coronary artery calcification score: analysis of the calcium acetate renagel comparison (CARE)-2 study. *Acad Radiol* 15:58–61
  14. Hausleiter J, Meyer T, Hermann F et al (2009) Estimated radiation dose associated with cardiac CT angiography. *JAMA J Am Med Assoc* 301:500–507
  15. Horiguchi J, Matsuura N, Yamamoto H et al (2009) Coronary artery calcium scoring on low-dose prospective electrocardiographically-triggered 64-slice CT. *Academic radiology* 16:187–193
  16. Mahnken AH, Wildberger JE, Simon J et al (2003) Detection of coronary calcifications: feasibility of dose reduction with a body weight-adapted examination protocol. *AJR Am J Roentgenol* 181:533–538
  17. Newton TD, Mehrez H, Wong K et al (2011) Radiation dose threshold for coronary artery calcium score with MDCT: how low can you go? *Eur Radiol* 21:2121–2129
  18. Shemesh J, Evron R, Koren-Morag N et al (2005) Coronary artery calcium measurement with multi-detector row CT and low radiation dose: comparison between 55 and 165 mAs. *Radiology* 236:810–814
  19. McNitt-Gray MF (2002) AAPM/RSNA Physics Tutorial for Residents: Topics in CT. Radiation dose in CT. *Radiographics* 22:1541–1553
  20. Takahashi N, Bae KT (2003) Quantification of coronary artery calcium with multi-detector row CT: assessing interscan variability with different tube currents pilot study. *Radiology* 228:101–106
  21. Bielak LF, Kaufmann RB, Moll PP et al (1994) Small lesions in the heart identified at electron beam CT: calcification or noise? *Radiology* 192:631–636
  22. Juri H, Matsuki M, Itou Y et al (2013) Initial experience with adaptive iterative dose reduction 3D to reduce radiation dose in computed tomographic urography. *J Comput Assist Tomogr* 37:52–57
  23. Tomizawa N, Nojo T, Akahane M et al (2012) Adaptive Iterative Dose Reduction in coronary CT angiography using 320-row CT: assessment of radiation dose reduction and image quality. *J Cardiovasc Comput Tomogr* 6:318–324
  24. Chen MY, Steigner ML, Leung SW et al (2013) Simulated 50% radiation dose reduction in coronary CT angiography using adaptive iterative dose reduction in three-dimensions (AIDR3D). *Int J Cardiovasc Imaging* 29:1167–1175
  25. van Osch JA, Mouden M, van Dalen JA et al (2014) Influence of iterative image reconstruction on CT-based calcium score measurements. *Int J Cardiovasc Imaging* 30:961–967
  26. Kurata A, Dharampal A, Dedic A et al (2013) Impact of iterative reconstruction on CT coronary calcium quantification. *Eur Radiol* 23:3246–3252
  27. McCollough CH, Ulzheimer S, Halliburton SS et al (2007) Coronary artery calcium: a multi-institutional, multimanufacturer international standard for quantification at cardiac CT. *Radiology* 243:527–538
  28. Horiguchi J, Matsuura N, Yamamoto H et al (2009) Effect of heart rate and body mass index on the interscan and interobserver variability of coronary artery calcium scoring at prospective ECG-triggered 64-slice CT. *Korean J Radiol* 10:340–346
  29. Matsuura N, Horiguchi J, Yamamoto H et al (2008) Optimal cardiac phase for coronary artery calcium scoring on single-source 64-MDCT scanner: least interscan variability and least motion artifacts. *AJR Am J Roentgenol* 190:1561–1568
  30. Achenbach S, Ropers D, Mohlenkamp S et al (2001) Variability of repeated coronary artery calcium measurements by electron beam tomography. *Am J Cardiol* 87:210–213
  31. Devries S, Wolfkiel C, Shah V et al (1995) Reproducibility of the measurement of coronary calcium with ultrafast computed tomography. *Am J Cardiol* 75:973–975